

P–C Bond Cleavage by a Heterobimetallic Polyhydrido Complex, $(C_5Me_5)Ru(\mu-H)_3Ir(C_5Me_5)$. Structure Determination and Fluxional Behavior of a Bridging Phosphido Complex, $(C_5Me_5)Ru(\mu-PPh_2)(\mu-H)(\mu-\eta^1:\eta^2-C_6H_5)Ir(C_5Me_5)$

Takanori Shima and Hiroharu Suzuki*

Department of Applied Chemistry, Graduate School of Science and Engineering, Tokyo Institute of Technology, O-okayama, Meguro-ku, Tokyo 152-8552, Japan

Received October 28, 2004

The heterobimetallic phosphido complex $(C_5Me_5)Ru(\mu-PPh_2)(\mu-H)(\mu-\eta^1:\eta^2-C_6H_5)Ir(C_5Me_5)$ (**2**) was formed by the reaction of $(C_5Me_5)Ru(\mu-H)_3Ir(C_5Me_5)$ (**1**) with triphenylphosphine as a result of P–C bond cleavage. The molecular structure of **2** was determined by single-crystal X-ray diffraction studies. The fluxional behavior of the $\mu-\eta^1:\eta^2$ -phenyl ligand in **2** was elucidated by means of a variable-temperature 1H NMR and a selective pulse irradiation method.

Introduction

We have recently demonstrated several typical examples of the site-selective coordination and activation of organic substrates by using heterobimetallic polyhydrido complexes, $(C_5Me_5)M(H)_3(\mu-H)_3Ru(C_5Me_5)$ ($M = Mo$ and W)¹ and $(C_5Me_5)Ru(\mu-H)_3Ir(C_5Me_5)$ (**1**),² as a precursor of the active species. For example, a σ -donor ligand has a tendency to be coordinated to the electron-deficient group VI metal rather than the ruthenium atom in the reaction of $(C_5Me_5)M(H)_3(\mu-H)_3Ru(C_5Me_5)$ ($M = Mo$ and W) with phosphine derivatives and amines.¹ Site-selective activation of ethylene took place when ethylene was treated with **1**. A divinyl complex, $(C_5Me_5)IrH(\mu-\eta^1:\eta^2-CH=CH_2)_2Ru(C_5Me_5)$, was exclusively formed probably as the result of site-selective C–H bond cleavage at the iridium center. In this reaction, the ruthenium center likely plays the role of a coordination site.²

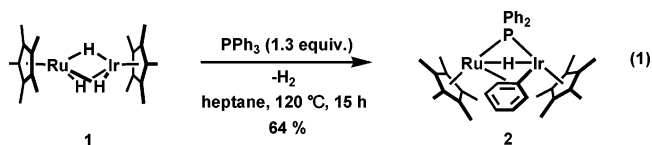
The introduction of a heterometal atom into a cluster core gives rise to an electronic anisotropy in the reaction field, and the reactivity would be influenced. Elucidation of the reactivity of the resulting heterometallic cluster would, therefore, be helpful for understanding the cooperative action of the metal centers in the cluster. The reactivity of structurally closely related homometallic clusters, $(C_5Me_5)Ru(\mu-H)_4Ru(C_5Me_5)$ and $(C_5Me_5)Ir(\mu-H)_2Ir(C_5Me_5)$, toward triphenylphosphine has been well established so far. The reaction of a dinuclear ruthenium tetrahydrido complex, $(C_5Me_5)Ru(\mu-H)_4Ru(C_5Me_5)$, with triphenylphosphine gave a stable dinuclear $\mu-\eta^2:\eta^2$ -benzene complex, $(C_5Me_5)Ru(\mu-PPh_2)(\mu-H)(\mu-\eta^2:\eta^2-C_6H_6)Ru(C_5Me_5)$, via P–C bond cleavage at the ruthenium center followed by the reductive coupling between the phenyl ligand and the hydride.³ On the

other hand, the reaction of a dinuclear iridium hydrido complex, $[(C_5Me_5)IrCl]_2(\mu-H)_2$, with triphenylphosphine selectively gave an *o*-phenylene complex, $(C_5Me_5)Ir(\mu-PPh_2)(\mu-H)(\mu-\eta^1:\eta^1-C_6H_4)Ir(C_5Me_5)$, as the result of successive P–C bond cleavage at each of the metal centers.⁴ The reaction mode of the heterometallic cluster, containing ruthenium and iridium, with triphenylphosphine is of considerable interest to understand the role allotted to individual metal atoms.

Here we report the structure determination and fluxional behavior of a novel heterobimetallic phosphido complex, $(C_5Me_5)Ru(\mu-PPh_2)(\mu-H)(\mu-\eta^1:\eta^2-C_6H_5)Ir(C_5Me_5)$ (**2**), exclusively formed in the reaction of **1** with triphenylphosphine.

Results and Discussion

Synthesis and Identification of a Heterobimetallic Complex Having a μ -Phosphido Ligand, $(C_5Me_5)Ru(\mu-PPh_2)(\mu-H)(\mu-\eta^1:\eta^2-C_6H_5)Ir(C_5Me_5)$ (2**).** Treatment of $(C_5Me_5)Ru(\mu-H)_3Ir(C_5Me_5)$ (**1**) with a slight excess of triphenylphosphine (1.3 equiv) in heptane at 120 °C for 15 h resulted in the formation of a heterobimetallic phosphido complex, $(C_5Me_5)Ru(\mu-PPh_2)(\mu-H)(\mu-\eta^1:\eta^2-C_6H_5)Ir(C_5Me_5)$ (**2**), as the result of P–C bond cleavage of triphenylphosphine at the iridium center (eq 1). Recrystallization from THF/MeOH afforded analytically pure **2** as black-red prisms in 64% yield.

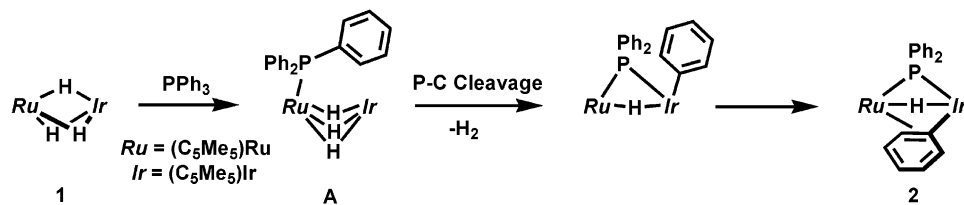


The structural identity of **2** was confirmed by means of 1H , ^{13}C , and ^{31}P NMR spectroscopy. The resonance for the bridging hydrido ligand of **2** appeared at δ –16.52 ppm as a doublet ($^2J_{PH} = 29.6$ Hz) due to the

* To whom correspondence should be addressed. E-mail: hiroharu@n.cc.titech.ac.jp. Tel: (+81)-3-5734-2148. Fax: (+81)-3-5734-3913.

(1) Shima, T.; Ito, J.; Suzuki, H. *Organometallics* 2001, 20, 10.

(2) Shima, T.; Suzuki, H. *Organometallics* 2000, 19, 2420.

Scheme 1. Formation of **2**

spin coupling with the ^{31}P nucleus. The chemical shift of the hydrido ligand is comparable to those observed for the diruthenium *ortho*-phenylene complex $(\text{C}_5\text{Me}_5)\text{Ir}(\mu\text{-PPh}_2)(\mu\text{-H})(\mu\text{-}\eta^1\text{:}\eta^1\text{-C}_6\text{H}_4)\text{Ir}(\text{C}_5\text{Me}_5)$ (**3**) (δ -17.7 ppm) and the diruthenium $(\text{C}_5\text{Me}_5)\text{Ru}(\mu\text{-PPh}_2)(\mu\text{-H})(\mu\text{-}\eta^2\text{:}\eta^2\text{-C}_6\text{H}_6)\text{Ru}(\text{C}_5\text{Me}_5)$ (**4**) (δ -16.6 ppm), and the $^2J_{\text{PH}}$ value of 29.6 Hz is almost the mean value of those observed for the above-mentioned diruthenium complex **3** and the diruthenium complex **4**, $^2J_{\text{PH}} = 18$ Hz and $^2J_{\text{PH}} = 40.6$ Hz, respectively.

The ^{31}P NMR spectrum of **2** revealed a resonance signal of the bridging phosphido ligand at δ 39.6 ppm. The ^{31}P signals for the bridging phosphido ligands typically range from δ 10 to 250 ppm,⁵ and the ^{31}P shifts for the phosphido ligand in homometallic complexes **3** and **4** are δ -5.0 and 168.0 ppm, respectively.

The phosphido complex **2** has a bridging phenyl ligand, σ -bonded to the iridium and π -bonded to the ruthenium centers, respectively, and the coordination mode of the aromatic C_6 -ligand in **2** is the mean of those represented in the diruthenium and the diruthenium analogues, **3** and **4**. The $(\text{C}_5\text{Me}_5)\text{Ru}(\mu\text{-PPh}_2)(\mu\text{-H})\text{Ir}(\text{C}_5\text{Me}_5)$ fragment in **2** is a 31e species, while the analogous homometallic fragments, $(\text{C}_5\text{Me}_5)\text{Ru}(\mu\text{-PPh}_2)(\mu\text{-H})\text{Ru}(\text{C}_5\text{Me}_5)$ and $(\text{C}_5\text{Me}_5)\text{Ir}(\mu\text{-PPh}_2)(\mu\text{-H})\text{Ir}(\text{C}_5\text{Me}_5)$, are 30e and 32e species, respectively. The difference in the number of valence electrons in the bimetallic $(\text{C}_5\text{Me}_5)\text{M}(\mu\text{-PPh}_2)(\mu\text{-H})\text{M}'(\text{C}_5\text{Me}_5)$ fragment influences the nature of the bonding interaction of the bridging phenyl group. The C_6 -ligands in **3** and **4** behave as a 2e-donor ($\mu\text{-}\eta^1\text{:}\eta^1\text{-mode}$) and a 4e-donor ($\mu\text{-}\eta^2\text{:}\eta^2\text{-mode}$), respectively. In contrast, the C_6 -ligand is coordinated as a 3e-donor ($\mu\text{-}\eta^1\text{:}\eta^2\text{-mode}$) in **2**.

The formation of **2** most likely proceeds, as depicted in Scheme 1, via an associative mechanism whereby the triphenylphosphine initially coordinates to the more electron-deficient ruthenium center.

Site-selective coordination of a tertiary phosphine ligand to the heterobimetallic cluster **1** has been also realized in the reaction with trialkylphosphines, such as PMe_3 and PEt_3 .⁶ Liberation of dihydrogen from intermediate **A** would induce coordination of one of the phenyl groups to the iridium center. Subsequent P–C bond cleavage at the iridium center, followed by coordination of the phenyl ligand to the ruthenium center, generates **2**. This mechanism is supported by the reaction of diruthenium tetrahydride, $(\text{C}_5\text{Me}_5)\text{Ru}(\mu\text{-H})_4$

$\text{Ru}(\text{C}_5\text{Me}_5)$, with tertiary phosphines. Previously, we reported that the reaction of the diruthenium tetrahydride with a series of trialkylphosphines resulted in the quantitative formation of a monophosphine complex, $(\text{C}_5\text{Me}_5)\text{Ru}(\text{PR}_3)(\mu\text{-H})_2\text{Ru}(\text{C}_5\text{Me}_5)$, which bears the phosphine ligand on one of the two ruthenium atoms.⁷ This result would justify the formation of intermediary species **A** in the initial stage of the reaction. In addition, a P–C(aryl) bond cleavage took place to yield an $\eta^2\text{:}\eta^2$ -arene phosphido complex, $(\text{C}_5\text{Me}_5)\text{Ru}(\mu\text{-}\eta^2\text{:}\eta^2\text{-arene})(\mu\text{-PRR}')(\mu\text{-H})\text{Ru}(\text{C}_5\text{Me}_5)$, exclusively in the reaction with an arylphosphine, $\text{P}(\text{Ar})\text{RR}'$.⁸

The most interesting feature of this reaction is the site-selectivity that the P–C bond cleavage exclusively takes place at the iridium center. Allotment of roles between the two metal centers would be facilitated in the heterobimetallic system in comparison to the homometallic one, probably due to polarization of the Ru–Ir bond. Such allotment of roles has been also observed in the reaction of **1** with ethylene; the ruthenium center and the iridium center play the role of a coordination site and an activation site, respectively, to form $(\text{C}_5\text{Me}_5)\text{IrH}(\mu\text{-}\eta^1\text{:}\eta^2\text{-CH=CH}_2)_2\text{Ru}(\text{C}_5\text{Me}_5)$, in which the vinyl ligands are σ -bonded to the iridium and π -bonded to the ruthenium.²

Molecular Structure of 2. The molecular structure of **2** was determined by X-ray crystallography and is shown in Figure 1 with the atom-labeling scheme. The

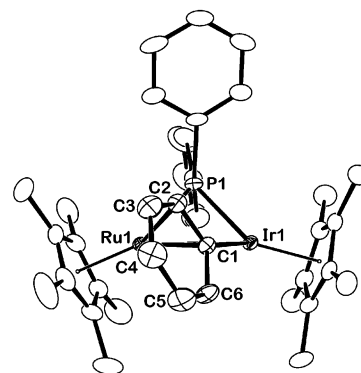


Figure 1. Molecular structure of $(\text{C}_5\text{Me}_5)\text{Ir}(\mu\text{-PPh}_2)(\mu\text{-H})(\mu\text{-}\eta^1\text{:}\eta^2\text{-C}_6\text{H}_5)\text{Ru}(\text{C}_5\text{Me}_5)$ (**2**). Bond lengths (Å) and angles (deg): Ir1–Ru1, 2.823(2); Ir1–C1, 2.076(6); Ru1–C1, 2.303(6); Ru1–C2, 2.552(6); Ir1–P1, 2.281(2); Ru1–P1, 2.304(2); C1–C2, 1.404(8); C2–C3, 1.415(9); C3–C4, 1.349(11); C4–C5, 1.390(12); C5–C6, 1.363(10); C6–C1, 1.424(9); Ir1–C1–C2 125.8(5), Ir1–C1–C6, 118.0(5), C2–C1–C6, 116.1(6); Ir1–P1–Ru1 76.01(6); Ir1–C1–Ru1, 80.11(19); Ru1–C1–C2, 83.2(4); Ru1–C2–C1, 63.7(3).

solid state structure is consistent with the NMR data. The diphenylphosphido group and the phenyl group

(3) Omori, H.; Suzuki, H.; Take, Y.; Moro-oka, Y. *Organometallics* **1989**, *8*, 2270.

(4) Grushin, V. V.; Vymenits, A. B.; Yanovsky, A. I.; Struchkov, Y. T.; Vol'pin, M. E. *Organometallics* **1991**, *10*, 48.

(5) (a) Petersen, J. L.; Stewart, R. P. *Inorg. Chem.* **1980**, *19*, 186.

(b) Carty, A. J.; MacLaughlin, S. A.; Taylor, N. J. *J. Organomet. Chem.* **1981**, *204*, C27. (c) Garrou, P. E. *Chem. Rev.* **1981**, *81*, 229. (d)

Johannsen, G.; Stetzer, O. *Chem. Ber.* **1977**, *110*, 3438. (e) Rosenberg, S.; Whittle, R. R.; Geoffroy, G. L. *J. Am. Chem. Soc.* **1984**, *106*, 5934.

(6) Shima, T.; Suzuki, H. Unpublished results.

(7) Ohki, Y.; Suzuki, H. *Angew. Chem., Int. Ed.* **2002**, *41*, 2994.

(8) Ohki, Y.; Suzuki, H. Manuscript in preparation.

bridge the ruthenium and the iridium. The ruthenium–iridium bond distance of 2.823 (2) Å is slightly shorter than the metal–metal separations in the homonuclear μ -phosphido complex of ruthenium (C₅Me₅)Ru(μ -PPh₂)(μ -H)(μ - η^2 : η^2 -C₆H₆)Ru(C₅Me₅) (2.945(1) Å) and iridium (C₅Me₅)Ir(μ -PPh₂)(μ -H)(μ - η^1 : η^1 -C₆H₄)Ir(C₅Me₅) (2.8901(4) Å). The EAN rule, when applied to **2**, requires a single bond between the ruthenium and the iridium. Although the Ru–Ir bond of **2** is somewhat short, it still lies in the range of a metal–metal single bond of the second-row transition metals. Ir1–P1 and Ru1–P1 bond lengths of 2.281(2) and 2.304(2) Å, respectively, are comparable to the Ir–P and the Ru–P bond lengths in the corresponding dinuclear μ -diphenylphosphido iridium and ruthenium complexes, (C₅Me₅)Ir(μ -PPh₂)(μ -H)(μ - η^1 : η^1 -C₆H₄)Ir(C₅Me₅) (2.263(2) Å) and (C₅Me₅)Ru(μ -PPh₂)(μ -H)(μ - η^2 : η^2 -C₆H₆)Ru(C₅Me₅) (2.307(2) Å). The Ir1–C1 bond distance of 2.076(6) Å is comparable to the Ir–C σ -bonds reported for mononuclear and dinuclear iridium complexes having a phenyl ligand, 2.063(7) Å for (η^5 -C₅Me₄Et)Ir(PMe₃)(C₆H₅)F⁹ and 2.054(7) Å for (C₅-Me₅)Ir(CO)(μ - η^1 : η^2 -*p*-C₆H₄OMe)(CO)Ir(C₅Me₅).¹⁰

Ru1–C1 and Ru1–C2 distances of 2.303(6) and 2.552(6) Å, respectively, are comparable to the π -bonded metal–carbon distances observed in the analogous μ - η^1 : η^2 -vinyl complex Ru₃(CO)₆(PPh₃)(μ - η^2 -C₆H₅)(μ -PPh₂)(μ_3 -S); Ru–C _{α} and Ru–C _{β} are 2.355(6) and 2.542(7) Å, respectively.¹¹ The C1–C2 bond length of 1.404(8) Å is significantly longer than that of the aromatic carbon–carbon double bond but is very similar to those reported for the transition metal η^2 - or η^2 : η^2 -arene complexes. In addition, the carbon–carbon bonds of the phenyl ring alternate in lengths. C3–C4 and C5–C6 distances are relatively short, 1.349(11) and 1.363(10) Å, respectively. On the basis of these results, we concluded that the C1–C2 bond of the phenyl group is π -coordinated to Ru1 in the solid state. The dihedral angle between the triangles Ru1–C1–C2 and C1–C2–C3 is 114.3(6)°, and this strongly supports the π -coordination of the C1–C2 bond to Ru1.

Dynamic Behavior of **2 in Solution.** While the phenyl ligand is coordinated in the μ - η^1 : η^2 -fashion in the solid state, it rotates around the Ir–C(*ipso*) bond in solution. A fluxional behavior of the bridging phenyl ligand was investigated by the variable-temperature ¹H NMR spectroscopy (Figure. 2).

In the ¹H NMR spectrum recorded at –120 °C, four signals attributable to the *para*-proton, *meta*-protons, and two kinds of *ortho*-protons of the bridging phenyl ligand appeared at δ 6.76, 6.31, and 7.23, and 5.11 ppm, respectively. These signals were unambiguously assigned on the basis of the ¹H,¹H-COSY spectrum. The *ortho*-proton observed at δ 5.11 ppm was assigned to the hydrogen attached to the carbon atom that participated in the η^2 -coordination to the ruthenium atom. The signal appearing at δ 7.23 ppm was due to the proton bonded to the uncoordinated *ortho*-carbon. The two signals of the *ortho*-protons broadened with an increase in the temperature and coalesced at –60 °C. The

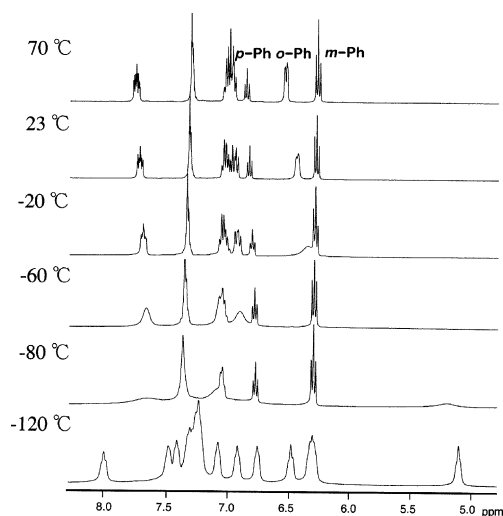


Figure 2. Variable-temperature 400 MHz ¹H NMR spectra (THF-*d*₈) of phenyl protons in **2**.

spectrum recorded at room temperature exhibited only three resonance signals at δ 6.29 (*meta*), 6.45 (*ortho*), and 6.84 (*para*) ppm for the phenyl ligand, and the signal of the *ortho*-protons sharpened to be observed as a doublet with intensity of 2H at 70 °C. The fact that the two *ortho*-protons were observed to be equivalent at higher temperature indicates that the phenyl ligand rapidly rotates around the Ir–C(*ipso*) bond in solution above room temperature. At low temperature, the rotation of the bridging phenyl ligand slowed, and one of the signals of the two *ortho*-protons shifts upfield probably due to coordination of the phenyl group to the ruthenium, and, as a result, the signals of the two *ortho*-protons were observed to be inequivalent at lower temperature. The ¹³C NMR spectrum recorded at low temperature also indicated the μ - η^2 -coordination of the phenyl ligand. A ¹³C NMR signal of one of the *ortho*-carbons of the phenyl ligand was observed at relatively high field, δ 102.5 ppm, as a doublet ($J_{CH} = 155.0$ Hz) at –100 °C.

Although the line-shape of the ¹H NMR signals for the phenyl ligand and the hydrides remained seemingly unchanged in the range from room temperature to about 100 °C, another mode of dynamic process, namely, exchange between the hydrido ligand and the *ortho*-hydrogen of the coordinated phenyl group, took place. This process was elucidated by a magnetization transfer experiment using the selective inversion recovery technique.¹²

A selective π pulse was applied at 100 °C to the resonance of the *ortho*-protons appearing at δ 6.58 ppm. Figure 3C is the difference spectrum obtained by recording a normal ¹H NMR spectrum (A) and subtracting a spectrum with irradiation of the π pulse at the frequency of the *ortho*-protons followed by a subsequent $\pi/2$ pulse after a delay time of 1.0 s (B).

For the mechanism of this dynamic process, we propose the following three candidates (Scheme 2). One of them involves orthometalation at the ruthenium center and a subsequent fast site exchange between the two hydrides (path A). The second one involves 1,2-shift

(9) Veltheer, J. E.; Burger, P.; Bergman, R. G. *J. Am. Chem. Soc.* **1995**, *117*, 12478.

(10) Yan, X.; Batchelor, R. J.; Einstein, F. W. B.; Zhang, X.; Nagelkerke, R.; Sutton, D. *Inorg. Chem.* **1997**, *36*, 1237.

(11) Hoferkamp, L. A.; Rheinwald, G.; Stoeckli-Evans, H.; Süss-Fink, G. *Organometallics* **1996**, *15*, 704.

(12) (a) Kalikhman, I.; Girshberg, O.; Lameyer, L.; Stalke, D.; Kost, D. *Organometallics* **2000**, *19*, 1927. (b) Blanca, M. B.-D.; Maison, E.; Kost, D. *Angew. Chem., Int. Ed. Engl.* **1997**, *36*, 2216.

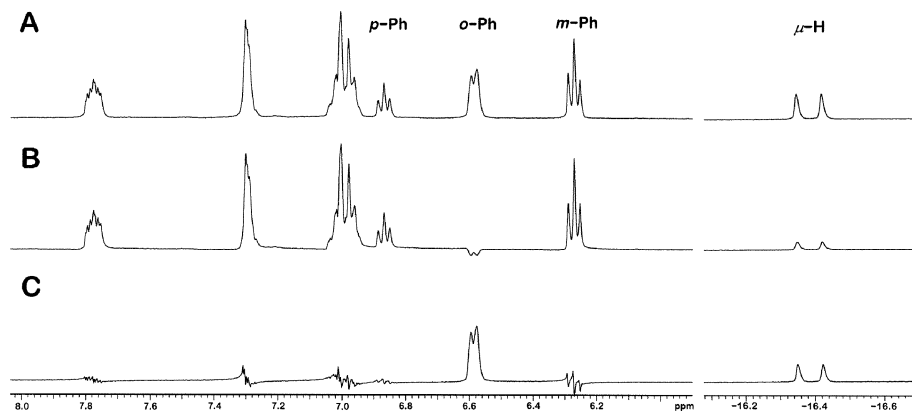
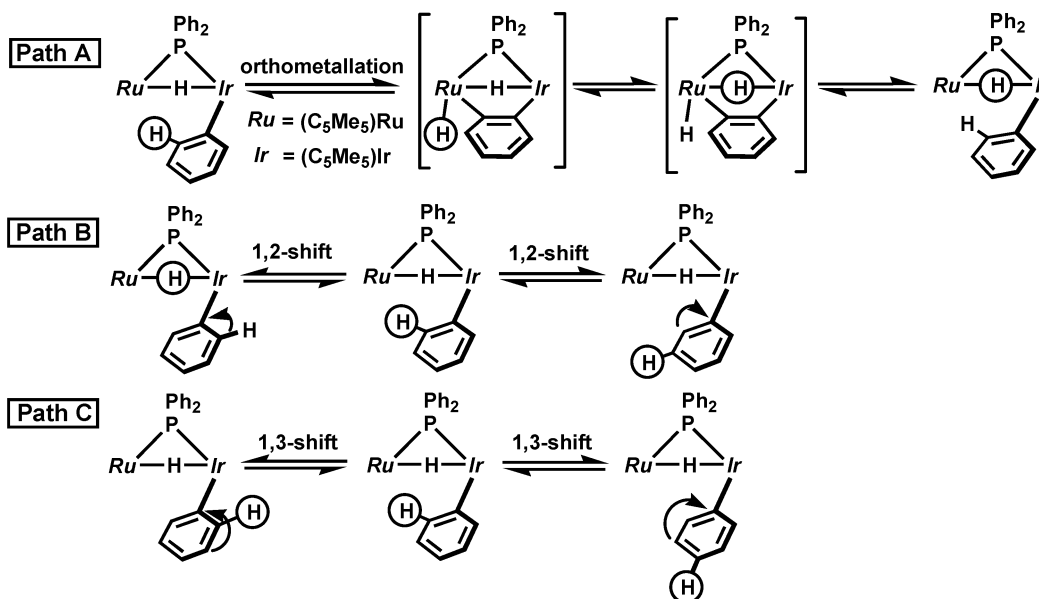


Figure 3. Magnetization transfer experiment of **2** (400 MHz ^1H NMR, $\text{THF-}d_8$, 100 $^\circ\text{C}$). (A) Normal ^1H NMR spectrum. (B) Spectrum with irradiation of the π pulse at the frequency of the *ortho*-protons followed by a subsequent $\pi/2$ pulse after a delay time of 1.0 s. (C) Difference spectrum obtained by recording spectrum A and subtracting spectrum B.

Scheme 2. Magnetization Transfer between the *ortho*-Proton and Hydrido Ligand



of the phenyl ring, which proceeds by way of an η^2 -benzene complex (path B).¹³ Third one involves 1,3-shift of the phenyl ring, which is analogous to the mechanism presented in many η^3 -benzyl complexes (path C).¹⁴

The spectra shown in Figure 3 definitely indicate the magnetization transfer from the *ortho*-proton to the hydrido ligand. In addition, no magnetization transfer to the hydrido ligand was observed when the *meta*-proton or *para*-proton resonance was irradiated. This implies that the magnetization transfer from the *ortho*-protons to the hydride does occur by way of path A. In contrast, path B should result in the exchange among the *ortho*- and *meta*-protons and the hydrido ligand. But the result of the NMR study was inconsistent with the experiment.¹⁵ Path C was also ruled out because the

magnetization transfer was not observed between the *ortho*- and the *para*-protons. It should be concluded from these results that the *ortho*-proton exchanges a bonding site with the hydride ligand via orthometallation.

Conclusion

A heterobimetallic polyhydrido complex, $(\text{C}_5\text{Me}_5)\text{Ru}(\mu\text{-H})_3\text{Ir}(\text{C}_5\text{Me}_5)$ (**1**), containing ruthenium and iridium reacts readily with PPh_3 to result in the exclusive formation of a bridging phosphido complex, $(\text{C}_5\text{Me}_5)\text{Ru}(\mu\text{-PPh}_2)(\mu\text{-H})(\mu\text{-}\eta^1\text{:}\eta^2\text{-C}_6\text{H}_5)\text{Ir}(\text{C}_5\text{Me}_5)$ (**2**), via the P–C bond cleavage. The X-ray diffraction study revealed that the phenyl ligand was π -bonded to the ruthenium and σ -bonded to the iridium centers. A fluxional behavior of the bridging phenyl ligand was exhibited by the variable-temperature ^1H NMR spectroscopy. The phenyl ligand, which is coordinated in the $\mu\text{-}\eta^1\text{:}\eta^2$ -fashion in solid state, rotates around the Ir–C(*ipso*) bond in solution. An exchange between the hydrido ligand and the *ortho*-hydrogen of the coordinated phenyl group was elucidated by a magnetization transfer experiment using the selective inversion recovery technique. The result strongly implied that the *ortho*-protons exchange

(13) (a) Jones, W. D.; Feher, F. J. *J. Am. Chem. Soc.* **1984**, *106*, 1650. (b) Jones, W. D.; Feher, F. J. *J. Am. Chem. Soc.* **1986**, *108*, 4814.

(14) (a) Mann, B. E. *Chem. Soc. Rev.* **1986**, *15*, 167. (b) Cotton, F. A.; Marks, T. J. *J. Am. Chem. Soc.* **1969**, *91*, 1339.

(15) Relaxation times (T_1) of the phenyl protons and the hydride in **2** at 80 $^\circ\text{C}$ in $\text{THF-}d_8$ are 3.52(1), 3.62(1), 4.44(1), and 4.32(2) s, for the *para*-H, *ortho*-H, *meta*-H, and the hydride, respectively. Therefore, the magnetization transfer between these protons should be observed by the measurement with a 1.0 s delay time if the exchange process exists among the *ortho*-H, the *meta*-H, and the hydride.

Table 1. Crystallographic Data for 2

formula	C ₃₈ H ₄₆ PRuIr	diffractometer	Rigaku AFC7R
cryst syst	monoclinic	radiation	Mo K α (λ = 0.71069 Å)
space group	P2 ₁ /c (#14)	monochromator	graphite
a, Å	15.880(10)	scan type	$\omega/2\theta$
b, Å	11.637(10)	2 θ_{\max}	55°
c, Å	18.663(7)	scan speed, deg/min	16.0
α , deg		no. of reflns collected	8042
β , deg	101.30(4)	no. of indep data	7766
γ , deg		no. of indep data ($I > 2\sigma(I)$)	6303
V, Å ³	3382(4)		
Z	4	R1	0.0440
D _{calcd} , g/cm ³	1.624	wR2	0.1163
temp, °C	-50.0	variables	380
μ , cm ⁻¹ (Mo K α)	44.49		

the bonding site with the hydride by way of a reversible orthometalation at the ruthenium center.

Experimental Section

General Procedures. All manipulations were carried out under an argon atmosphere with use of standard Schlenk techniques. Toluene, Et₂O, and THF were distilled from sodium benzophenone ketyl prior to use. Pentane was dried over P₂O₅ and distilled prior to use. Methanol was dried over Mg(OMe)₂ and distilled prior to use. (C₅Me₅)Ru(μ -H)₃Ir(C₅Me₅) (**1**)² was prepared according to a previously published method. Other reagents were used as received. IR spectra were recorded on a Nicolet Avatar 360 FT-IR and Jasco FT/IR-5000 spectrometer. ¹H, ¹³C, and ³¹P NMR spectra were recorded on Varian INOVA-400 Fourier transform spectrometers with tetramethylsilanes or H₃PO₄ 85% as an internal or external standard. Elemental analyses were recorded on a Perkin-Elmer 2400II.

X-ray Data Collection and Reduction. Crystals suitable for X-ray analysis of **2** were obtained from a pentane solution at 0 °C. The crystals were mounted on glass fibers. The data were collected on a Rigaku AFC-7R four-circle diffractometer equipped with graphite-monochromated Mo K α radiation (λ = 0.71069 Å) in the 5° < 2 θ < 55° range. The data were processed using the TEXSAN crystal structure analysis package¹⁶ operated on an IRIS Indigo computer. At the early stages of the refinement, the atomic scattering factors were obtained from the standard sources. In the reduction of the data, Lorentz/polarization corrections and empirical absorption corrections based on azimuthal scans were applied to the data for each structure.

Structure Solutions and Refinement. The structures were solved by the Patterson method (DIRDIF94¹⁷ PATTY¹⁸) and expanded using Fourier techniques. The non-hydrogen atoms were refined by full-matrix least-squares on F^2 using the SHELXL-97 program systems.¹⁹ All hydrogen atoms were located by difference Fourier maps and refined isotropically. Crystal data and results of the analyses are listed in Table 1.

Selective Pulse Irradiation in 2. Selective pulse technique is easily applied to slow chemical exchange in small diamagnetic molecular systems using Varian INOVA 400 Pandora's Box (pbox) software. This software creates radio frequency (rf) pattern files for experiments involving a shaped rf pulse sequence which consists of the long selective π pulse, followed by a short observation pulse after various delay times, to examine the effect of the selective pulse on line intensities.

(16) TEXSAN, Crystal Structure Analysis Package; Molecular Structure Corp.: The Woodlands, TX, 1985 and 1992.

(17) Beurskens, P. T.; Admiraal, G.; Beurskens, G.; Bosman, W. P.; de Gelder, R.; Israel, R.; Smits, J. M. M. *DIRDIF94*; University of Nijmegen: The Netherlands, 1994.

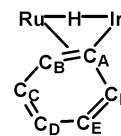
(18) Beurskens, P. T.; Admiraal, G.; Beurskens, G.; Bosman, W. P.; Garcia-Granda, S.; Gould, R. O.; Smits, J. M. M.; Smykalla, C. *PATTY*; University of Nijmegen: The Netherlands, 1992.

(19) Sheldrick, G. M. *SHELXL-97*, Program for Crystal Structure Solution; University of Goettingen: Germany, 1997.

Selective pulse irradiation in **2** was performed in flame-sealed NMR tubes in THF-*d*₈ at 100 °C by using the *ortho*-Ph (δ 6.45) or hydride signals (δ -16.67) according to previously published procedures.¹² There was no chemical exchange between the Ph proton and hydride if the selective π pulse was applied to the *meta*-Ph (δ 6.29) or *para*-Ph (δ 6.84) signals. The data in Figure 3 were obtained by applying the selective π pulse to the *ortho*-Ph signal.

(C₅Me₅)Ru(μ -PPh₂)(μ -H)(μ - η^1 - η^2 -C₆H₅)Ir(C₅Me₅) (2**).** A 50 mL glass autoclave was charged with 239.1 mg (0.422 mmol) of (C₅Me₅)Ru(μ -H)₃Ir(C₅Me₅) (**1**), 140.0 mg (0.533 mmol) of PPh₃, and 5 mL of heptane. After stirring for 15 h at 120 °C, the color of the solution changed from red-brown to red. Removal of the solvent under reduced pressure and crystallization from THF/MeOH at -30 °C gave 221.2 mg (0.268 mmol, 64%) of **2** as black-red crystals. ¹H NMR (400 MHz, THF-*d*₈, rt, δ /ppm): 7.73 (m, 2 H, PPh₂), 7.33 (m, 3 H, PPh₂), 6.99 (m, 5 H, PPh₂), 6.84 (t, J_{HH} = 7.2 Hz, 1 H, *Ir-para*-Ph), 6.45 (d, J_{HH} = 5.2 Hz, 2 H, *Ir-ortho*-Ph), 6.29 (t, J_{HH} = 7.2 Hz, 2 H, *Ir-meta*-Ph), 1.87 (s, 15 H, C₅Me₅), 1.45 (d, J_{PH} = 1.6 Hz, 15 H, C₅Me₅), -16.52 (d, J_{PH} = 29.6 Hz, 1 H, μ -H). ¹³C NMR (100 MHz, C₆D₆, rt, δ /ppm): 144.6 (d, J_{PC} = 36.4 Hz, Ph), 136.1 (dd, J_{PC} = 9.9 Hz, J_{CH} = 158.3 Hz, Ph), 134.1 (dd, J_{PC} = 11.4 Hz, J_{CH} = 160.3 Hz, Ph), 133.1 (d, J_{PC} = 21.2 Hz, Ph), 127.9 (d, obscured by C₆D₆, Ph), 126.8 (dd, J_{PC} = 9.8 Hz, obscured by C₆D₆, Ph), 126.4 (dd, J_{PC} = 2.3 Hz, obscured by C₆D₆, Ph), 125.4 (d, J_{CH} = 151.7 Hz, Ph), 124.0 (d, J_{CH} = 155.6 Hz, Ph), 101.3 (s, *Ir-Ph*), 92.8 (d, J_{PC} = 1.6 Hz, C₅Me₅), 82.3 (d, J_{PC} = 1.5 Hz, C₅Me₅), 11.1 (q, J_{CH} = 125.6 Hz, C₅Me₅), 10.4 (q, J_{CH} = 126.1 Hz, C₅Me₅). ³¹P NMR (162 MHz, C₆D₆, rt, H₃PO₄ 85%, δ /ppm): 39.6. IR (KBr) 3058, 2908, 1584, 1570, 1481, 1435, 1377, 1025, 969, 741, 725, 698 cm⁻¹. Anal. Calcd for C₃₈H₄₆PRuIr: C, 55.19; H, 5.57. Found: C, 55.42; H, 5.72.

Variable-Temperature NMR Spectra of 2. Variable-temperature NMR study of **2** was performed in flame-sealed



NMR tubes in THF-*d*₈ using a Varian INOVA-400 Fourier transform spectrometer with tetramethylsilane as an internal standard. ¹H NMR (400 MHz, THF-*d*₈, -120 °C, δ /ppm): 8.01 (s, 1 H, Ph), 7.49 (s, 1 H, Ph), 7.42 (s, 1 H, Ph), 7.24 (m, 4 H, Ph), 7.23 (1 H, C_F), 7.08 (s, 1 H, Ph), 6.92 (s, 1 H, Ph), 6.76 (s, 1 H, C_D-H), 6.49 (s, 1 H, Ph), 6.31 (s, 2 H, C_C-H and C_E-H), 5.11 (s, 1 H, C_B-H), 1.89 (s, 15 H, C₅Me₅), 1.45 (s, 15 H, C₅Me₅), -16.67 (d, J_{PH} = 30.4 Hz, 1 H, μ -H). ¹³C NMR (100 MHz, THF-*d*₈, -100 °C, δ /ppm): 153.8 (d, J_{CH} = 156.9 Hz, Ph), 145.3 (d, J_{PC} = 37.1 Hz, Ph), 136.9 (m, Ph), 134.1 (m, Ph), 129.7 (m, Ph), 128.2 (m, Ph), 124.3 (d, J_{CH} = 159.3 Hz, Ph), 121.4 (d, J_{CH} = 156.2 Hz, Ph), 104.5 (s, C_A), 102.5 (d, J_{CH} = 155.0 Hz, C_B), 94.2 (s, C₅Me₅), 84.0 (s, C₅Me₅), 12.3 (q, J_{CH} = 125.4 Hz, C₅Me₅), 11.6 (q, J_{CH} = 125.9 Hz, C₅Me₅).

Acknowledgment. This work was supported by a Grant-in-Aid for Scientific Research (Grant Nos. 1520-5009 and 14078101, “Reaction Control of Dynamic Complexes”) from the Ministry of Education, Culture, Sports, Science and Technology of Japan and partially supported by the 21st Century COE Program. The authors are also grateful to Kanto Chemical Co., Inc., for a generous supply of pentamethylcyclopentadiene.

Supporting Information Available: $^1\text{H},^1\text{H}$ COSY spectra of **2** at $-100\text{ }^\circ\text{C}$, tables of atomic coordinates and thermal parameters, bond lengths and angles, torsion angles, and structure refinement details, and ORTEP drawing of **2** with full numbering scheme. This material is available free of charge via the Internet at <http://pubs.acs.org>.

OM049162K